RSC Advances

ROYAL SOCIETY OF CHEMISTRY

www.rsc.org/advances

PAPER

Preparation and application of magnetic graphene oxide coated with a modified chitosan pH-sensitive hydrogel: An efficient biocompatible adsorbent for catechin

Hassan Sereshti*, Soheila Samadi, Shohreh Asgari, Maryam Karimi

In the present study, graft copolymerization of acrylic acid sodium salt (AAS) onto *O*-carboxymethyl chitosan (*O*-CMCs) produced a highly hydrophilic and pH-sensitive hydrogel polymer of *O*-CMCs-g-AAS with a porous surface morphology. The grafted chitosan copolymer was coated on magnetic graphene oxide (MGO) and characterized with TEM, SEM, and FT-IR techniques. The prepared nanocomposite, [*O*-CMCs-g-AAS]/MGO, was successfully used as an efficient and biocompatible adsorbent in a magnetic solid phase extraction (MSPE) coupled with gas chromatography-mass spectrometry (GC-MS) for preconcentration and determination of catechin in tea beverage. Influence of the main parameters affecting quality of the coating process was investigated and optimized using a response surface methodology. Under the optimum conditions, the adsorbent demonstrated a satisfactory adsorption capacity (27 mg g^{-1}) for catechin and good linearity in the range of 0.005-5 μg mL^{-1} with determination coefficient (R^2) of 0.9987. The limit of detection (LOD) and limit of quantification (LOQ) were 0.001 and 0.003 μg mL^{-1}, respectively. The relative standard deviation (RSD) was 4.1% (n=5, C=0.5 μg mL^{-1}). The abstract should be a single paragraph which summarises the content of the article.

Introduction

Since a report by Geim and Novoselov[1] graphene (G) has been attracting great interest due to its unique structure and characteristics.[2-4] Other forms of graphene-based materials, such as graphene oxide (GO), reduced graphene oxide (rGO), and exfoliated graphite, have been reliably produced in large scale. The promising properties together with the ease of processibility and functionalization make graphene-related materials ideal candidates for incorporation into a variety of functional materials.[5] Graphene with a double-sided polyaromatic framework and an huge specific surface area (theoretically 2630 m^2 g^{-1}), is a promising adsorbent with high loading capacity. Its large delocalized π-electron system also provides G a strong affinity for carbon-based ring structures, which are widely present in drugs, pollutants, and biomolecules. The solid phase extraction (SPE) is a powerful tool for preconcentration and purification of analyte(s) from a great variety of sample matrices. Regarding the superior characteristics and high chemical stability of G, it can be employed as an ideal adsorbent for SPE. However, the direct use of G or GO as SPE adsorbent has several problems that can be reduced with functionalization and surface modification.[6] In the past decade, magnetic nanocomposite (MNC) materials have attracted much attention in various scientific fields such as biotechnology, biomedicine, and environmental and material science. The MNC adsorbents, with large surface area and high adsorption capacity, can be quickly isolated from sample solutions by applying an external magnetic field. Thus, the difficulties of solid-liquid separation or the high back-pressure when passing through the SPE column are avoided.[7,8] The MGO nanosheets are highly oxygenated graphene derivatives (with hydroxyl, epoxide, diol, ketone and carboxyl functional groups and Fe_3O_4 nanoparticles) that the van der Waals interactions in them has altered to hydrogen bonding or electrostatic interactions. Therefore, they are more compatible with organic polymers containing oxygen and nitrogen functional groups.[9-12]

Chitosan (Cs) is a linear polysaccharide composed of randomly distributed β-(1-4)-linked and D-glucosamine and N-acetyl-D-glucosamine units.[13] Due to its nontoxicity, biocompatibility, and biodegradability, Cs has been extensively used in various fields, such as biomaterials, textile, drug delivery, environmental protection, and metallurgy.[14] The active hydroxyl and amino groups on the chitosan molecules favor the development of different chemical-derived modifications with tailored physical and chemical properties that different from those of chitosan.[7,15] Graft copolymerization of chitosan is a useful technique for modifying its chemical and physical properties.[16] The primary derivatization (*O*-carboxymethylation) of chitosan, before graft copolymerization, results in much improved water solubility and bioactivities. *O*-Carboxymethyl-chitosan grafted with acrylic acid sodium salt (*O*-CMCs-g-AAS) was generated a porous, water soluble and hydrogel copolymer. The polyacrylate side-chains are protonated at low pH values, and thus the polymer is cross-linked to form a pH-sensitive hydrogel.

A hydrogel is a network of hydrophilic polymers cross-linked by covalent bonds, hydrogen bonding, van der Waals interactions, or physical entanglements.[17] Hydrogels can absorb large quantities of water while maintaining their structure.[18] They might be functionalized with different groups such as carboxylic acid, amine, hydroxyl, and sulfonic acid.[19] Because of the advantages

such as great adsorption rate and capacity, hydrogels have been used for the removal of pollutants from aqueous solution[20-24] and in the development of the smart drug delivery systems. They can protect the drug from hostile environments, e.g. the presence of enzymes and low pH in the stomach. Hydrogels can also control drug release by changing the gel structure in response to environmental stimuli.[18]

Catechin (Figure 1) is a biologically active polyphenol found in tea leaves and has various applications in food and pharmaceutical industries for their valuable properties mostly as antioxidant.[25,26] The antiallergic and inhibitory effects of catechin on deoxyribonucleic acid (DNA) polymerase activity, human cancer cell growth, and inflammation have also been studied.[27]

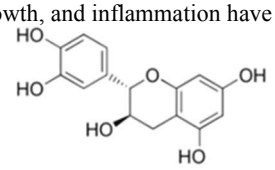

Figure 1. Chemical structure of catechin.

In the present work, we synthesized GO-Fe_3O_4 nanocomposite and a biocompatible chitosan-based copolymer (*O*-CMCs-g-AAS). Then, the synthesized MGO was coated with *O*-CMCs-g-AAS, and thus an adsorbent with a porous hydrophilic layer containing many active functional groups was obtained. Afterward, the prepared adsorbent was used by applying MSPE method for preconcentration of catechin in water and tea samples. The porosity and net-like coating of the adsorbent acted as a barrier to natural organic matters in complex matrices such as tea without influencing the adsorption of the analytes.[7]

EXPERIMENTAL SECTION

Reagents and materials

All chemicals, including iron(III) chloride hexahydrate ($FeCl_3.6H_2O$), iron(II) chloride tetrahydrate ($FeCl_2.4H_2O$), acrylic acid, tert-butyl methyl ether (MTBE), formic acid (FA) and ferrous ammonium sulfate hexahydrate ($(NH_4)_2Fe(SO_4)_2.6H_2O$), all in analytical grade were purchased from Merck Chemicals (Darmstadt, Germany). Sodium acrylate was prepared with the addition of NaOH (1.67 g) to aqueous solution of acrylic acid (2 mL in 9 mL distilled water). Chitosan (MW 7.9×10^5, degree of deacetylation 92%) was obtained from Hangzhou New Asia International (Hangzhou, China). Catechin (≥99.0 %) was purchased from Fluka (Buchs, St. Gallen, Switzerland). Derivatization reagent: N-methyl-N-(trimethylsiliyl) trifluoroacetamide (MSTFA) containing 1% trimethylchlorosilne (TMCS) was purchased from Sigma Aldrich (St Louis, MO, USA). Graphite powder was supplied from Samchung Pure Chemical (Pyeongtaek, Korea). Stock standard solution of catechin (1000 μg mL^{-1}) was prepared in water, stored under refrigeration and protected from light. Working standard solutions were prepared by diluting the stock standard solutions and kept at 4 °C before use. Double distilled water was used in all experiments.

Preparation of MGO

Graphite oxide was synthesized by a modified Hummers method.[28] Briefly, 1 g of $NaNO_3$ and 1 g of graphite powder were added to 50 mL 98% H_2SO_4 in a 500 mL three-neck flask. The mixture was placed in an ice bath with stirring. Then, 6 g of $KMnO_4$ was slowly added to the mixture and the temperature maintained less than 10 °C for 1 h. Thereafter, the reaction was transferred to a 40 °C oil bath and stirred for 24 h. Then, 40 mL water was gradually added to it, causing an increase in temperature. After dilution with 140 mL of H_2O, 10 mL of 30 % H_2O_2 was added to the mixture. The brown sediment was washed with sufficient HCl (5%) and distilled water until the pH became neutral. Then, the rinsed product was dispersed in deionized water using ultrasound for 30 min, and finally air-dried under ambient conditions.

Magnetic graphene oxide was prepared by chemical coprecipitation method.[29] First, GO (0.04 g) was dispersed in 40 mL of water by sonication for 30 min. Under a nitrogen atmosphere and vigorous stirring, 0.2 g of $FeCl_3.6H_2O$ and 0.075 g of $FeCl_2.4H_2O$ in 50 mL of water were slowly added to the mixture. The temperature of the mixture was increased to 80-85 °C and then NH_4OH solution (25%) was added dropwise to it until pH reached to about 11. After 45 min, the temperature was decreased and the black sediment was washed by deionized water for three times and dried under ambient conditions.

Preparation of *O*-CMCs-g-AAS

O-Carboxymethyl chitosan (*O*-CMCs) was prepared according to the method described by Liu et al.[30] 0.3 g of *O*-CMCs and 9 mL of sodium acrylate (3 M) with 7 mL of water were charged into a small reactor. Then, 0.01 g of $(NH_4)_2Fe(SO_4)_2$ dissolved in 2 mL H_2O_2 was slowly added to the reactor content as an initiator, and the total volume of the reaction mixture was made up to 20 mL with water. Therewith, N_2 (g) was bubbled through the solution for 30 min to remove the dissolved oxygen. The reaction was performed at a constant temperature (70 °C) for 2 h. Afterward, the reaction product was precipitated in an excess of acetone, filtered to remove the supernatant liquid, and finally washed with sufficient EtOH to eliminate the unreacted *O*-CMCs and ferrous salt. Then, the obtained product was extracted with EtOH for 48 h and dried. The copolymerization of *O*-CMCs with sodium acrylate greatly improved water solubility of chitosan. The graft copolymerization of sodium acrylate on *O*-CMCs is shown in Figure 2.

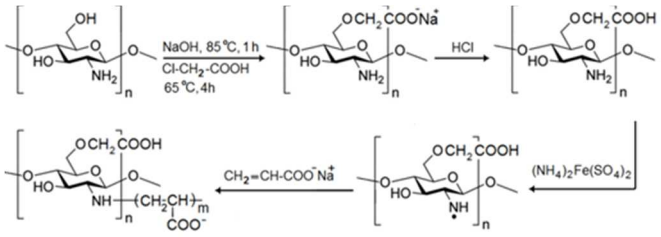

Figure 2. The preparation scheme for *O*-carboxymethyl-chitosan grafted-acrylic acid sodium salt (*O*-CMCs-g-AAS) copolymer.

Coating of MGO with *O*-CMCs-g-AAS

150 mg of MGO was dispersed in 40 mL water using ultrasonication, and then 40 mL of an aqueous solution containing 47 mg of *O*-CMCs-g-AAS was added to it. The mixture was shaken by a mechanical stirrer at 150 rpm in an oil

bath for 20 h at 26 ºC. Thereafter, the product was rinsed three times with water and air-dried under ambient conditions.

Instruments

The morphology of MGO, *O*-CMCs-g-AAS, and [*O*-CMCs-g-AAS]/MGO was investigated by a transmission electron microscopy (TEM, Philips CM30 machine, Netherlands) at an accelerating voltage of 150 kV, and a scanning electron microscopy (SEM, S-4160 Hitachi, Tokyo, Japan) operating at 20 kV. Fourier transform-infrared (FT-IR) transmittance spectra were taken using a Bruker Equinox 55 FT-IR spectrometer (Bremen, Germany) as potassium bromide (KBr) pellets. Zeta potentials were determined with nanobrook zetaPALS (Brookhaven USA).

Gas chromatography

Flavanols such as catechins are the major flavonoids that have been analyzed by gas chromatography (GC). GC coupled with mass spectrometric detection offers a sensitive and accurate tool for quantitative and qualitative flavonoid analysis. The analysis of flavonoids by GC usually involves the main stages including: sample extraction, derivatization and GC analysis.[27] The chromatography analyses were carried out using an Agilent technologies GC-MS (Santa Clara CA, USA) consisted of a 6890 GC system coupled with a 5973 network mass selective detector and equipped with a HP5-MS capillary fused silica column (length, 30 m; internal diameter, 0.25 mm; film thicknesses, 0.25 µm; and stationary phase, (5% phenyl)-methyl polysiloxane). The performed GC temperature program was as follows: the initial temperature was set at 160 ºC and maintained for 1 min, then was programmed at 30 ºC min^{-1} to 270 ºC and maintained for 10 min. The injection port temperature was set at 230 ºC and was performed in splitless mode (time, 1 min). Other operating conditions were: carrier gas, He (99.999%) with a flow rate of 1 mL min^{-1}. An enhanced Chemstation G1701 DA version D.00.01.27 was used for the data collection and processing. Mass spectra were taken at 70 eV ionization energy and full scan mode. The scanned mass range and the solvent delay time were set at 50-800 m/z and 6 min, respectively.

Extraction procedure

At first, 20 mg of the synthesized adsorbent ([*O*-CMCs-g-AAS]/MGO) was conditioned with MeOH (1 mL) and water (2 mL). Then, 5 mL of a standard solution of catechin (0.5 µg mL^{-1}) was added to it. Then, the mixture was shaken for 30 min at the rate of 300 rpm to equilibrate the adsorption process. Subsequently, the solid phase was collected by an external strong magnet and rinsed by water (1 mL). In the next step, the adsorbed catechin was eluted from the adsorbent using 500 µL of MTBE/MeOH/FA (4.5:4.5:1, v/v/v) with 5 min shaking. After phase separation, the eluent was evaporated to dryness under a gentle stream of N_2 (g).

Derivatization of catechin

The trimethylsiliyl derivatives of flavonoids such as catechin are preferred for qualitative and quantitative GC analysis. This process improves the volatility, peak shapes, detection limit, and quantitative reproducibility of these compounds for GC analysis.[27] For this purpose, the extracted catechin obtained from the previous section was resolved in 50 µL of the derivatization reagent using vortexing for 30 s, and then was incubated at 60 ºC for 60 min. The derivatization reagent (MSTFA) yields only one derivatized product with higher signal intensity.[31] Finally, the mixture was cooled and an aliquot of 1 µL was injected into the GC-MS system.

Results and discussion

Characterization of [*O*-CMCs-g-AAS]/MGO

The SEM and TEM images of *O*-CMCs, *O*-CMCs-g-AAS, MGO and [*O*-CMCs-g-AAS]/MGO are shown in Figure 3. Figures 3a and 3b demonstrate that the flaky and fibrous surface morphology of *O*-CMCs has been changed to a porous structure after the grafting process. Figure 3c exhibits the Fe_3O_4 nanoparticles with the mean size of about 50 nm were precipitated on the GO nanosheets successfully. The TEM image in Figure 3d displays the homogeneous coating of the grafted chitosan on MGO.

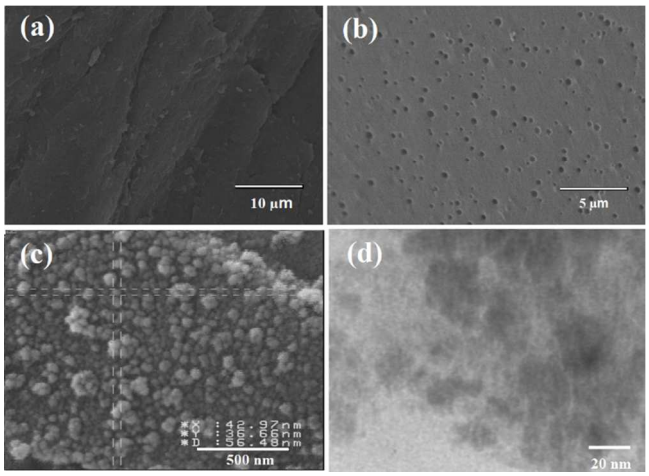

Figure 3. SEM images of a) *O*-carboxymethyl chitosan (*O*-CMCs), b) *O*-CMCs grafted with acrylic acid sodium salt (*O*-CMCs-g-AAS), c) magnetic graphene oxide (MGO), and d) TEM image of [*O*-CMCs-g-AAS]/MGO (the adsorbent).

The synthesis of Fe_3O_4, the attachment of Fe_3O_4 nanoparticles on the GO nanosheets surface, and the coating of [*O*-CMCs-g-AAS] on MGO were evidenced with FT-IR spectra in Figure 4. The peaks at 564 and 522 cm^{-1} in Figures 4a and 4b related to the Fe-O group prove the existence of Fe_3O_4 nanoparticles in MGO and the adsorbent ([*O*-CMCs-g-AAS]/MGO). Figure 4c shows the FT-IR spectrum of the polymeric coating of the adsorbent (*O*-CMCs-g-AAS). The peak at 2927 cm^{-1} corresponds to saturated C-H stretching absorption. The strong band at 1562 cm^{-1} and the medium intensity band at 1403 cm^{-1} could be ascribed to asymmetric and symmetric vibrations of carboxylate groups of polyacrylate chains, respectively. The broad band at 3300-3500 cm^{-1} was attributed to the stretching vibration of O-H, extension vibration of N-H, and inter-hydrogen bonds of the polysaccharide.[7] The band at 1708 cm^{-1} could be attributed to the C=O stretching vibration in *O*-carboxymethyl group of chitosan. The bands at 1175 and 1043 cm^{-1} are associated with the C-O stretching vibrations.

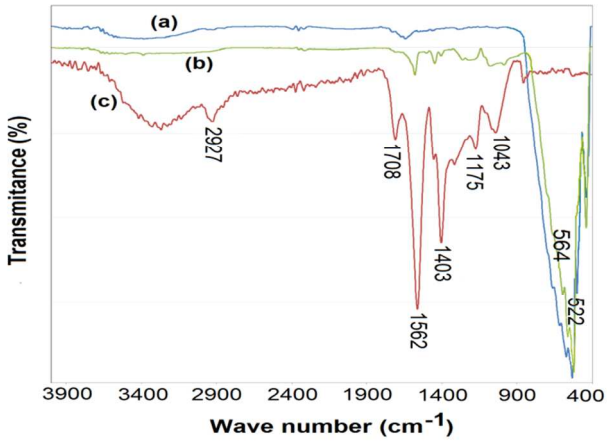

Figure 4. FT-IR spectra of: (a) Fe_3O_4-graphene oxide (MGO), (b) the adsorbent ([*O*-CMCs-g-AAS]/MGO), and (c) O-carboxymethyl chitosan grafted with acrylic acid sodium salt (*O*-CMCs-g-AAS).

Optimization of the coating process

The adsorption of catechin molecules on [*O*-CMCs-g-AAS]/MGO depends on the quality of coating of *O*-CMCs-g-AAS on MGO nanosheets. Therefore, in order to achieve the best conditions for the adsorption of catechin, the significant factors influencing the yield of the procedure, including temperature of the coating process (20-50 °C), the contact time between MGO and *O*-CMCs-g-AAS (4-24 h), and the *O*-CMCs-g-AAS dosage (20-150 mg) were investigated and optimized using a central composite design (CCD).[32] A CCD is composed of a 2^n factorial design, 2n star points (α-levels), and *m* replications of the center point. The number of required experiments *N* needed for CCD can be calculated with equation (1):

$$N=2^n+2n+m \quad (1)$$

where *n* is the number of variables. The design center points were obtained equal to nine, resulting in a total of 23 experiments. The experiments were executed in random order to minimize the effect of uncontrolled factor. The adsorption (%) of catechin by the synthesized magnetic nanocomposite was chosen as the response variable and calculated using equation (2):

$$\text{Adsorption}\% = \frac{C_o - C_e}{C_o} \times 100 \quad (2)$$

where C_o and C_e are the initial and equilibrium concentrations of catechin in the sample solution. In order to evaluate the efficiency of the adsorbent, the product of each experiment was tested in accordance to the following procedure. 20 mg of the obtained adsorbent was conditioned with MeOH (1 mL) and water (2 mL). Then, 5 mL of standard solution of catechin (50 μg mL^{-1}) was added to it and shaken at 300 rpm for 30 min. Then, the magnetic adsorbent was separated from the solution using an external magnetic field, and the equilibrium concentration of catechin (C_e) was detected using UV-Vis spectrophotometry at 279 nm (λ_{max} of catechin). After performing the experiments, a quadratic polynomial regression model based on the experimental data and in term of coded values was generated (equation (3)).

$$Y=77.53+3.13t-3.64T-5.12M-1.27tT-0.85tM+1.98TM-0.31t^2-1.85T^2-2.39M^2 \quad (3)$$

where Y is the response (adsorption percent of catechin). The statistical significance of the model and the precision were justified by analysis of variance (ANOVA). According to the ANOVA (Table 1), t, T, M, TM, T^2, and M^2 are significant model terms. Therefore, the effect of temperature and *O*-CMCs-g-AAS dosage (TM) as the effective interaction on the adsorption of catechin can be represented as the surface plot (Figure 5). The temperature demonstrates a quadratic effect on the response; hence the adsorption (%) of catechin increases up to a maximum of about 86.5% at 26 °C. Moreover, the *O*-CMCs-g-AAS dosage also displays a quadratic effect on the response yielding a maximum of about 87% at 45 mg. Regarding these explanations, the optimum conditions of the coating process were calculated based on the equation (2) as: 20 h for time, 26 °C for temperature and 47 mg for amount of the adsorbent (0.6 mg mL^{-1}) with the maximum response amount (E%) of about 89%.

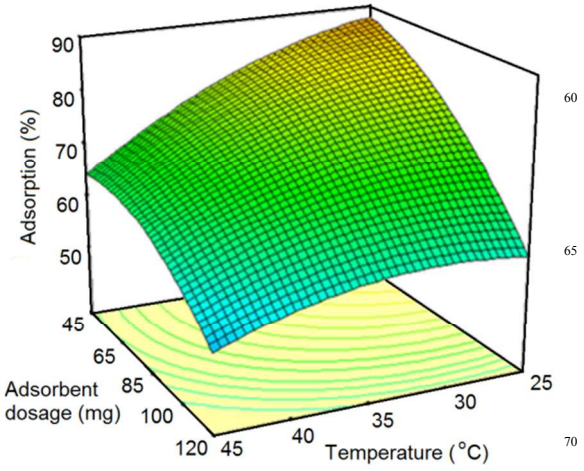

Figure 5. Response surface plot for the effect of adsorbent dosage and temperature on the adsorption (%).

Effect of salt addition

The adding salt to aqueous sample solutions can affect the performance of adsorption. Depending on the composition of the solution and nature of the analyte(s), it may have different effects such as aggregation, increasing, decreasing or no change on the adsorption efficiency.[33,34] The influence of salt concentration on the adsorption of catechin was investigated by adding 0-10%, w/v of NaCl into the aqueous sample solution while the other parameters were fixed constant during adsorption. When 7 % (w/v) NaCl was added at the beginning of the extraction, the adsorption was almost constant. For further investigation, the salt was added to the sample solution in the middle of shaking. The results showed that the adsorption increased about 4% with increasing of salt concentration from 0 to 7%, and then the adsorption decreased with adding more salt (up to 10%). Therefore, since the addition of salt had no marked effect on the adsorption of catechin and also for simplicity of the procedure, the addition of salt was neglected.

Effect of the solution pH

The stability and the chemical form of catechins are highly influenced by the solution pH. Generally, catechins are stable in acidic pH conditions. With increasing the pH value, their stability decreases through *cis-trans* isomerization and oxidative degradation.[35,36] On the other hand, the surface charge and functionality of the adsorbent, which is controlled by the pH of the solution, plays a very important role in the adsorption process. Therefore, zeta potential of the adsorbent in aqueous solution at pH 3-7 was determined. As shown in Figure 6, pH_{pzc} was equal to 5.2. At pH<5.2, the adsorbent surface is positively charged (because the carboxylate groups on the acrylate chains are protonated) and at pH>5.2 the negative surface charge is attributed to the deprotonation of these groups.[24] In order to find the optimum pH value at which the adsorption capacity is the maximum, the adsorption of catechin at the pH values of 6.1 (natural pH of the sample solution), 3 and 8 were studied. The solution pH was adjusted to the required values with 0.1M HNO_3 and 0.1M NaOH. The results revealed that with changing the surface potential from -36.9 mV at pH 6.1 to +35.4 mV at pH 3, the adsorption was nearly constant (±0.75%). However, at pH values higher than 6.1 that negative surface charge increases, the adsorption capacity decreased to about 3%. This fact can be attributed to the degradation of catechin in this conditions.[36] Regarding the above mentioned explanations, it can be concluded that the electrostatic interactions between catechin and the adsorbent do not plays a significant role in the adsorption process. Therefore, because catechin is stable in acidic conditions and the adsorption in this region is almost constant, in order to avoid the complexity of the procedure, the pH of sample solution (pH 6.1) was chosen as the optimum pH value for further experiments.

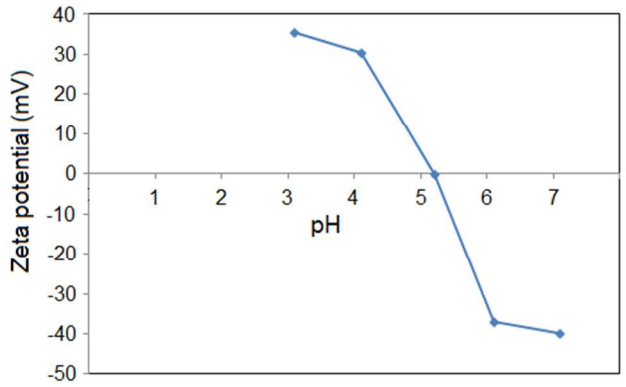

Figure 6. The effect of pH on the surface charge of the adsorbent ([*O*-CMCs-g-AAS]/MGO). The measurements were performed in the aqueous solutions containing 1 mg of the adsorbent per mL.

O-CMCs-g-AAS is a cross-linked polymeric pH-sensitive hydrogel. The carboxylate groups on polyacrylate side-chains of the chitosan backbone are protonated at low pH values. The hydrogen bonding between these protonated groups results in the cross linking of the side chains. This property was investigated in the pH range of 1.5-10. Figure 7 shows clearly that the solutions at pH 2-3 become turbid because of the insoluble hydrogel formation.

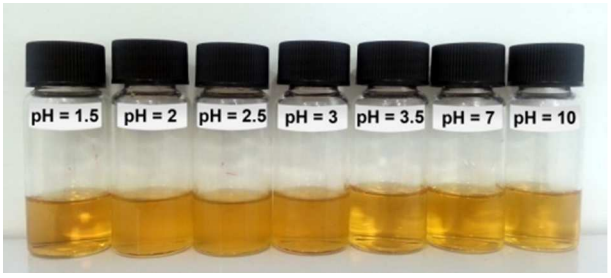

Figure 7. Effect of pH (1.5-10) on the cross-linking of O-carboxymethyl chitosan-g-acrylic acid sodium salt (*O*-CMCs-g-AAS). The solutions became turbid at pH 2, 2.5 and 3, due to the formation of the insoluble hydrogel network (cross-linked *O*-CMCs-g-AAS).

Influence of adsorption time

The effect of adsorption time on the quantitative adsorption of catechin was studied by varying the contact time of [*O*-CMCs-g-AAS]/MGO with the aqueous solution of catechin in the range of 10-50 min. Figure 8 shows that the adsorption yield of catechin increased with increasing the adsorption time up to 40 min, and remained almost constant with further increase. For adsorption times higher than 30 min, the slope reduces gradually and, moreover, this causes the procedure to be prolonged. Therefore, 30 min was selected as the optimum adsorption time for further experiments.

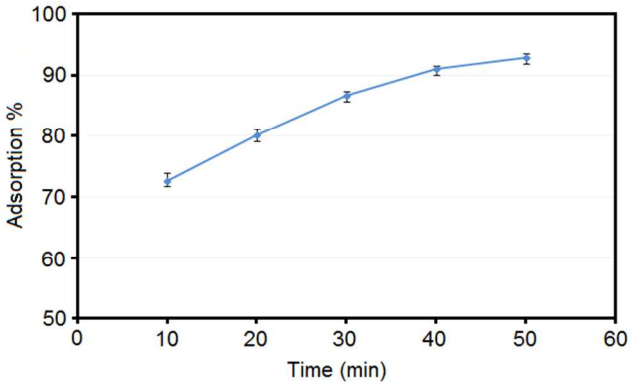

Figure 8. Effect of adsorption time on the adsorption of catechin. Conditions: sample solution, 5 mL; adsorption dosage, 20 mg; pH, 6.1.

Elution solvent

The efficiency of desorption is highly dependent on the solvent used for the elution. In order to select an appropriate elution solvent, MeOH and several mixed-solvent systems containing methanol such as MeOH/0.1 M HNO_3 (1:1, v/v) pH 1.4, MeOH/1 M AcH (2:1, v/v) pH 3.3 and MTBE/MeOH/FA (4.5:4.5:1, v/v/v) pH 1.5 were tested by the proposed procedure.[27,31] MeOH is a protic solvent that can disrupt hydrogen bonding between catechin and the adsorbent. In addition, the acidic conditions favor the stability of catechin. The results showed that among these solvents, MTBE/MeOH/FA exhibited a significantly higher desorption yield. Therefore, it was chosen as the preferred desorption solvent for further experiments (Figure 9).

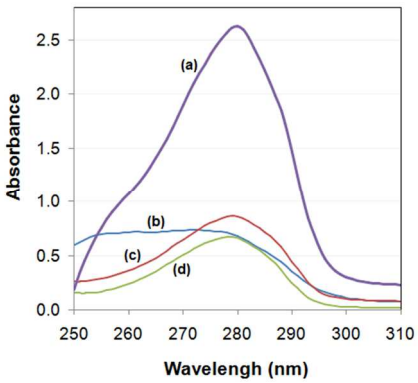

Figure 9. The UV-Vis absorbance spectra of catechin in: (a) MTBE/MeOH/FA, (b) MeOH/HNO_3, and (c) MeOH/AcH; (d) standard solution of catechin in water (50 μg mL^{-1}). MTBE (methyl tert-butyl ether); MeOH (methanol); FA (formic acid); HNO_3 (nitric acid); AcH (acetic acid).

Mechanism of adsorption

The contribution of the adsorbent components to the adsorption process was investigated by comparison of the adsorption of catechin (the analyte), phenol and resorcinol. Phenol and resorcinol (both similar to catechin composed of benzene ring with hydroxyl functional groups) were selected as model compounds to study the nature of interaction between the adsorbent and catechin. The experiments were carried out using 5 mL aliquots of the standard solutions (50 mg L^{-1}) of these compounds with the proposed procedure. In order to evaluate the adsorption efficiency, the equilibrium concentration of these compounds was detected using UV-Vis spectrophotometry at 279, 270, and 273 nm (λ_{max} of catechin, phenol and resorcinol, respectively), and the adsorption percent was calculated by equation (2). Moreover, the zeta potentials (ζ) were determined to study the influence of surface charge on the adsorption. The following conclusions can be drawn from the results obtained (Table 2): (i) the adsorption of catechin on the adsorbent was not influenced by the surface charge of the adsorbent; (ii) the adsorption affinity toward the adsorbent was enhanced with increasing the number of hydroxyl groups on the compounds. The possible adsorption interactions between the analytes and the adsorbent can be of hydrogen bonding and anion-π interactions; (iii), MGO plays the main role in the adsorption process, and the coating (*O*-CMCs-g-AAS) with the surface charge of -36.9 mV (due to the presence of carboxylic groups) prevents the agglomeration of the MGO nanosheets and improves the dispersion of the adsorbent particles in the sample solution. These results led to improvement in the efficiency and RSDs. The porosity and net-like coating of the adsorbent acted as a barrier to natural organic matters in complex matrices such as tea without influencing the adsorption of the analytes.

Method validation

Under the optimum operating conditions, the analytical figures of merit consisted of linear dynamic range (LDR), limit of detection (LOD), determination coefficient (R^2) and relative standard deviation (RSD%) for determination of catechin were estimated for validation of the proposed method. The calibration curve was constructed in accordance with the proposed procedure using a collection of different catechin standard solutions (5 mL) with the concentration levels in the range of 0.005-5.0 μg mL^{-1} and was characterized with the determination coefficient (R^2) of 0.9987. The LOD based on $3S_d/m$ (S_d and m are the standard deviation of the blank and the slope of calibration graph, respectively), was equal to 0.001 μg mL^{-1}. The LOQ calculated with formula $10S_d/m$ was 0.003 μg mL^{-1}. The precision of the method (RSD%) was assessed by performing five replicates analysis of a catechin standard solution (0.5 μg mL^{-1}) equal to 4.1%.

Table 2. Adsorption (%) ± standard deviation (SD) of some phenolic compounds with different adsorbents to investigate contribution of the adsorbent components on the adsorption capacity.

Adsorbent	pH[a]	Catechin	Resorcinol	Phenol	ζ[a] (mV)
O-CMCs-g-AAS/MGO	6.1	87.3±0.5	47.1±0.7	24.0±0.4	-36.9
MGO	4.7	72.2±1.9	39.7±2.5	22.2±3.6	31.4
O-CMCs-g-AAS/Fe_3O_4	5.9	37.5±1.0	<2	<2	-23.2
Fe_3O_4	5.4	92.3±1.5	<2	<2	24.8
O-CMCs-g-AAS	7.1	-	-	-	-15.9

[a] The measurements were performed in the aqueous solution containing 1 mg of the adsorbent per mL.

Adsorption capacity

The capacity of the adsorbent is an important factor that determines the amount of adsorbent required for the adsorption of a specific amount of analyte from the solution quantitatively. For investigation of adsorption capacity of [*O*-CMCs-g-AAS]/MGO, aliquots of 5 mL of sample solution with different concentration levels of catechin were contacted with 20 mg of the adsorbent in accordance with the proposed procedure. The equilibrium adsorption capacity (Q_e) was calculated using equation (4):

$$Q_e = \frac{(C_0 - C_e)V}{m} \quad (4)$$

where *V* is the volume of the catechin solution (L), and *m* is the weight of the adsorbent (g). The adsorption isotherm that describes the mass-transfer equilibrium of catechin between the adsorbent and the solution is shown in Figure 10. According to the results, the maximum amount of catechin that can be adsorbed on [*O*-CMCs-g-AAS]/MGO was found to be 27 mg g^{-1}.

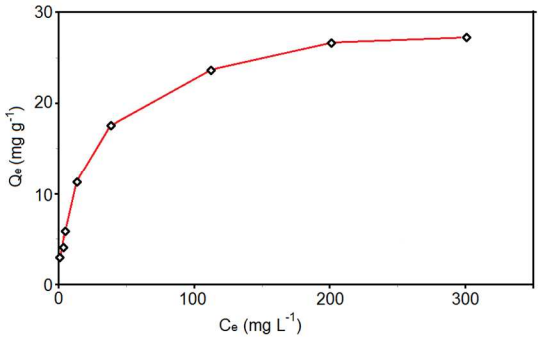

Figure 10. The adsorption isotherm of catechin on [*O*-CMCs-g-AAS]/MGO. Conditions: catechin (C_0), 5-400 mg L^{-1}; sample solution, 5 mL; adsorption dosage, 20 mg; pH, 6.1; and time, 30 min.

Analysis of real samples

The applicability of the method for determination of catechin in commercial green and black teas was evaluated using the proposed procedure under the optimum conditions. Since, tea is rich in catechins and is also popular non-alcoholic beverages; they were selected as real samples for analysis by the presented method. For this purpose, 20 mg of the tea sample (previously ground and homogenized) was placed in a 100 mL beaker and 20 mL of boiling distilled water was added to it (1 mg mL^{-1}). The mixture was kept at 70 ºC for 10 min, and then the solid particles were removed from the mixture using an appropriate filter paper. Then, 5 mL of this solution was used for determination of catechin according to the procedure, without further pretreatment. The matrix effect on the recovery of catechin was also investigated by spiking a known concentration of catechin into the tea samples and the recovery of catechin was determined. The results obtained from the analysis of the non-spiked and spiked real samples given in Table 3 demonstrate that the sample matrices had no significant effect on the adsorption efficiency of catechin. The GC-MS chromatograms obtained for green and black tea samples using [*O*-CMCs-g-AAS]/MGO as adsorbent in MSPE under the optimum conditions were shown in Figure 11. The identification of TMS derivatives of catechin and epicatechin was confirmed by comparison of their mass spectra with those stored on Wiley7n.l MS computer library. Epicatechin was also quantified using the calibration curve of catechin as 5336 ng mL^{-1} ± 3.4 (RSD %) in green tea and 2125 ng mL^{-1} ± 3.8 (RSD %) in black tea sample.

Table 3. Mean detected concentration (ng mL^{-1}) ± RSD (n=3) of catechin found in commercial green and black teas, and the relative recoveries ± RSD (n=3) of the spiked samples with standard solution of catechin (400 ng mL^{-1}).

Sample	Catechin ± RSD	RR (%) ± RSD
Green tea	554 ± 4.0	96.2 ± 4.3
Black tea	981 ± 3.7	97.5 ± 3.8

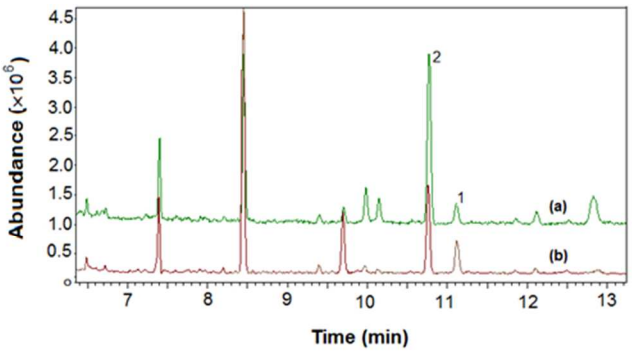

Figure 11. The GC-MS chromatograms of: (a) green tea and (b) black tea beverages obtained by the proposed method. Catechin (1) and epicatechin (2) were identified and marked as their TMS derivatives in the chromatograms as a result of derivatization prior to GC-MS analysis.

Conclusion

A simple extraction (MSPE) method using a green adsorbent composed of MGO nanosheets coated with a hydrogel chitosan-based copolymer (*O*-CMCs-g-AAS) was developed for preconcentration of catechin in tea samples. The coating process was optimized using a central composite design. Using the optimized conditions, an adsorption capacity of 27 mg g^{-1}, a low detection limit (0.001 µg mL^{-1}) and a relatively wide linear dynamic range (10^3) were obtained. The extraction procedure is eco-friendly because it consumes small volume of organic solvent (500 µL) and requires low sample volume (5 mL).

Since, the adsorbent, composed of MGO and the chitosan copolymer, used in this work is a biocompatible, biodegradable and nontoxic [24,37] and in addition, catechins are important components of tea with many biological functions including anti-inflammatory, anti-oxidative and anti-carcinogenic effects, the authors propose that the prepared adsorbent can be used in the catechin delivery in biological fluids. The porous and net-like morphology of the adsorbent prevents the macromolecules in complex matrices to pass through it readily and thus enhances the selectivity of the adsorbent toward catechins. Moreover, the magnetic property, water dispersability and ultra-high surface area of the adsorbent provide a simple operation for an efficient drug loading and controlled release mechanism.[38,39] In addition, *O*-CMCs-g-AAS is a cross-linked polymeric pH-sensitive hydrogel (at pH 2-3). This type of hydrogels has been most frequently used to develop controlled release formulations for oral administration.[18]

Acknowledgment

The authors gratefully acknowledge Ms. Ghazaleh Aliakbarzadeh and Mr. Mohammad Ahmadvand for helping us to prepare the graphical abstract and description of adsorbent structure.

Notes and references

[a] *Department of Chemistry, Faculty of Science, University of Tehran, P.O. Box 14155-64555, Tehran, Iran. Fax: +98 21 66495291; Tel: +98 21 61113632; E-mail: sereshti@khayam.ut.ac.ir (H. Sereshti).*

† Electronic Supplementary Information (ESI) available: [details of any supplementary information available should be included here]. See DOI: 10.1039/b000000x/

1 K. S. Novoselov, A. K. Geim, S. V. Morozov, D. Jiang, Y. Zhang, S. V. Dubonos, I. V. Grigorieva and A. A. Firsov, *Science*, 2004, **306**, 666.
2 A. K. Geim and K. S. Novoselov, *Nat. Mater.*, 2007, **6**, 183.
3 Y. Zhu, S. Murali, W. Cai, X. Li, J. W. Suk, J. R. Potts and R. S. Ruoff, *Adv. Mater.*, 2010, **22**, 3906.
4 Q. Liu, J. Shi and G. Jiang, *TrAC, Trends Anal. Chem.*, 2012, **37**, 1.
5 X. Huang, Z. Yin, S. Wu, X. Qi, Q. He, Q. Zhang, Q. Yan, F. Boey and H. Zhang, *Small*, 2011, **14**, 1876.
6 Q. Liu, J. Shi, J. Sun, T. Wang, L. Zeng and G. Jiang, *Angew. Chem. Int. Ed*, 2011, **50**, 5913.
7 X. Zhang, H. Niu, Y. Pan, Y. Shi and Y Cai, *Anal. Chem.*, 2010, **82**, 2363.
8 X. S. Li, G. T. Zhu, Y. B. Luo, B. F. Yuan and Y. Q. Feng, *TrAC, Trends Anal. Chem.*, 2013, **45**, 233.
9 T. Kuilla, S. Bhadra, D. Yao, N. H. Kim, S. Bose and J. H. Lee, *Prog. Polym. Sci.*, 2010, **35**, 1350.
10 J. Du and H. M. Cheng, *Macromol. Chem. Phys.*, 2012, **213**, 1060.
11 H. J. Salavagione, G. Martinez and G. Ellis, *Macromol. Rapid Commun.*, 2011, **32**, 1771.
12 R. Sitko, B. Zawisza and E. Malicka, *TrAC, Trends Anal. Chem.*, 2013, **51**, 33.
13 N. Bhattarai, J. Gunn and M. Zhang, *Adv. Drug Deliver. Rev.*, 2011, **62**, 83.
14 L. Liu, C. Li, C. Bao, Q. Jia, P. Xiao, X. Liu and Q. Zhang, *Talanta*, 2012, **93**, 350.

15 A. Zhu, L. Yuan and Sh. J. Dai, *Phys. Chem. C*, 2008, **112**, 5432.
16 J. M. Joshi and V. K. Sinha, *J. Polym. Research*, 2006, **13**, 387.
17 K. Kamath and K. Park, *Adv. Drug Deliv. Rev.*, 1993, **11**, 59.
18 Y. Qiu and K. Park, *Adv. Drug Deliver. Rev.*, 2012, **64**, 49.
19 Q. Wang, X. Xie, X. Zhang, J. Zhang and A. Wang, *Int. J. Biol. Macromol.,* 2010, **46**, 356.
20 A.T. Paulino, M.R. Guilherme, A.V. Reis, G.M. Campese, E.C. Muniz and J. Nozaki, *J. Colloid Interface Sci.,* 2006, **301**, 55.
21 E.K. Yetimoğlu, M.V. Kahraman, G. Bayramoğlu, Ö. Ercan and N.K. Apohan, *Radiat. Phys. Chem.,* 2009, **78**, 1800.
22 Y. Zheng, J. Zhang and A. Wang, *Chem. Eng. J.,* 2009, **155**, 215.
23 Y. Liu, Y. Zheng and A. Wang, *J. Environ. Sci.*, 2010, **22**, 486.
24 Y. Zheng, D. Huang and A. Wang, *Anal. Chim. Acta*, 2011, **687**, 193.
25 H. Tanaka, H. Miyoshi, Y. C. Chuang, Y. Ando and T. Takahashi, *Angew. Chem. Int. Ed*, 2007, **46**, 5934.
26 P. Gogoi, S. Hazarika, N. N. Dutta and P. G. Rao, *Chem. Eng. J.*, 2009, **155**, 810.
27 Y. Nolvachai and P. J. Marriott, *J. Sep. Sci.*, 2013, **36**, 20.
28 W. S. Hummers and R. E. Offeman, *J. Am. Chem. Soc.*, 1958, **80**, 1339.
29 M. Z. Kassaee, E. Motamedi and M. Majdi, *Chem. Eng. J.*, 2011, **172**, 540.
30 X. F. Liu, Y. L. Guan, D. Z. Yang, Z. Li and K. D. Yao, *J. Appl. Polym. Sci.*, 2001, **79**, 1324.
31 S. Magiera, C. Uhlschmied, M. Rainer, Ch. W. Huck, I. Baranowska and G. K. Bonn, *J. Pharmaceut. Biomed.*, 2011, **56**, 93.
32 M.A. Bezerra, R.E. Santelli, E.P. Oliveira, L.S. Villar and L.A. Escaleira, *Talanta*, 2008, **76**, 965.
33 Y. Zhang and H. K. Lee, *J. Chromatogr. A*, 2012, **1249**, 25.
34 J. Li, D. Kuang, Y. Feng, F. Zhang, Z. Xu, M. Liu and D. Wang, *Biosens. Bioelectron.*, 2013, **42**, 198.
35 N. Li, L. S. Taylor, M. G. Ferruzzi and L. J. Mauer, *J. Agric. Food Chem.*, 2012, **60(51)**, 12531.
36 H. Horie and K. Kohata, *J. Chromatogr. A*, 2000, **881**, 425.
37 M. Yang, J. Yao and Y. Duan, *Analyst*, 2013, **138**, 72.
38 H. Hu, C. Tang and C. Yin, *Mater. Lett.*, 2014, **125**, 82.
39 Y. Chen, Y. Qi, X. Yan, H. Ma, J. Chen, B. Liu and Q. Xue, *J. Appl. Polym. Sci.*, 2014, **131**, 1.

PAPER

Table 1 Analysis of variance table (ANOVA) for response surface quadratic model.

Source [a]	Sum of squares [b]	d.f. [c]	Mean square [d]	F-value [e]	p-value, prob>F [f]	Significance
Model	5.655×10^{11}	12	4.713×10^{10}	350.69	<0.0001	significant
t	3.933×10^{10}	1	3.933×10^{10}	292.69	<0.0001	
T	1.818×10^{10}	1	1.818×10^{10}	135.3	<0.0001	
E	3.409×10^{11}	1	3.409×10^{11}	2536.59	<0.0001	
S	1.704×10^{8}	1	1.704×10^{8}	1.27	0.3112	
tT	7.992×10^{8}	1	7.992×10^{8}	5.95	0.0588	
E	3.986×10^{9}	1	3.986×10^{9}	29.66	0.0028	
tS	2.746×10^{9}	1	2.746×10^{9}	20.43	0.0063	
TE	1.781×10^{10}	1	1.781×10^{10}	132.52	<0.0001	
t^2	2.213×10^{9}	1	2.213×10^{9}	16.46	0.0098	
T^2	9.124×10^{9}	1	9.124×10^{9}	67.9	0.0004	
E^2	1.822×10^{11}	1	1.822×10^{11}	1355.77	<0.0001	
S^2	3.244×10^{9}	1	3.244×10^{9}	24.14	0.0044	
Residual [g]	6.719×10^{8}	5	1.344×10^{8}			
Lack of fit [h]	3.318×10^{8}	2	1.659×10^{8}	1.46	0.3601	not significant
Pure error [i]	3.401×10^{8}	3	1.134×10^{8}			
CorTotal [j]	8.688×10^{11}	22				

[a] Source of variation. [b] Sum of the squared differences between the average values and the overall mean. [c] Degrees of freedom. [d] Sum of squares divided by d.f. [e] Test for comparing term variance with residual (error) variance. [f] Probability of seeing the observed F-value if the null hypothesis is true. [g] Consists of terms used to estimate experimental error. [h] Variation of the data around the fitted model. [I] Variation in the response in replicated design points. [j] Totals of all information corrected for the mean.

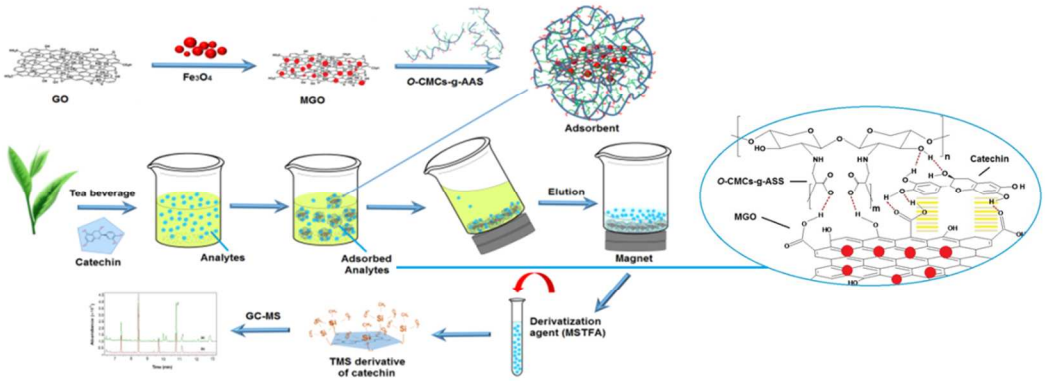

Graphical abstract (scheme)

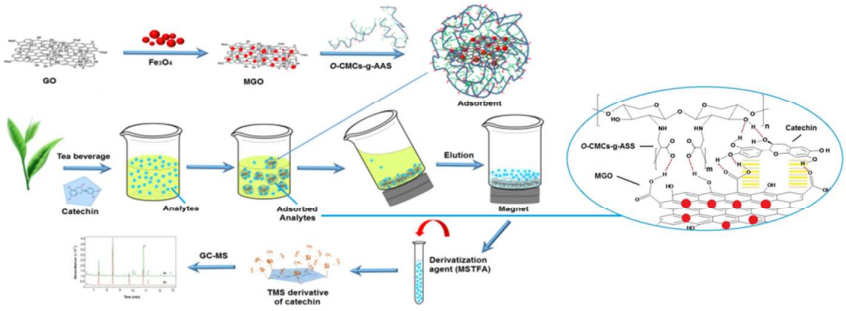

A MSPE method using a pH-sensitive green chitosan-based adsorbent coupled with GC-MS developed for determination of catechin in tea samples.